13th International Conference on Applications of Statistics and Probability in Civil Engineering, ICASP13
Seoul, South Korea, May 26-30, 2019

Updated robust reliability: considering record-to-record variability and uncertainty in modelling parameters

Fatemeh Jalayer
Associate Professor, Dept. of Structures for Engineering and Architecture, University of Naples "Federico II", Naples, Italy

Hossein Ebrahimian
Assistant Professor, Dept. of Structures for Engineering and Architecture, University of Naples "Federico II", Naples, Italy

ABSTRACT: Modeling parameter uncertainty can affect significantly the structural seismic reliability assessment. However, this type of uncertainty may not be described by a Poisson process as it lacks renewal properties with the occurrence of each earthquake event. Furthermore, considering uncertainties related to ground motion representation by employing as-recorded ground motions together with modeling parameter uncertainties can prove quite challenging. Robust fragility assessment, proposed previously by the authors, employs the structural response to recorded ground motion as data in order to update prescribed seismic fragility models. Robust fragility can be extremely efficient for considering also the structural modelling uncertainties by creating a dataset of one-to-one assignments of structural model realizations and as-recorded ground motions. This can reduce the computational effort by about two orders of magnitude. However, it should be kept in mind that the fragility concept is based on the underlying assumption of Poisson-type renewal. Using the concept of updated robust reliability, considering both uncertainty in ground motion representation based on as-recorded ground motion and non-ergodic uncertainties, the conservative error introduced by adopting Poissonian structural reliability assessment based on the robust fragility concept can be quantified.

INTRODUCTION

The concept of average fragility, first introduced for probabilistic risk assessment of the nuclear power plants (Kennedy and Ravindra 1983), considers the uncertainty in the estimation of median for a Lognormal fragility model. By treating the results of structural analysis for a suite of ground motion records as data and by employing the Bayesian inference, one can propagate the uncertainties in the parameters of a given fragility model. This technique which is dubbed as "robust fragility" (Jalayer et al. 2015, 2017), inspired from the concept of updated robust reliability (Papadimitriou et al. 2001, Beck and Au 2002), can provide an extremely efficient way for considering the modeling uncertainties, record-to-record variability and the limited sample size (Miano et al. 2017).

However, the concept of fragility itself is implicitly built upon a Poissonian stochastic description of the uncertain parameters, which does not seem to be suitable for describing the uncertainties which do not renew after occurrence of each earthquake event (non-ergodic uncertainties, Der Kiureghian 2005). Thus, it is important to quantify the error introduced by using the fragility curves for describing both the record-to-record variability and the non-ergodic

uncertainties. This paper strives to propagate the uncertainties in a prescribed fragility model parameters and the structural modelling parameter uncertainties for the more general case in which the fragility concept is applied only to the "Poissonian" or the ergodic subset of the uncertain parameters in the problem (e.g., those related to earthquake occurrence). The results are compared to the "equivalent" robust fragility used for describing both ergodic and non-ergodic uncertainties. This is done for a bi-dimensional MDOF frame of an existing older RC school building designed for gravity loading only (in its pre-retrofit state).

1. METHODOLOGY

The uncertainty propagation here is studied in the context of the PEER performance-based framework.

1.1. The Intensity Measure (IM) and the Structural Damage Measure

First-mode spectral acceleration denoted by $S_a(T_1)$ or simply S_a is adopted herein as the intensity measure. Recently, many researchers have focused on *IM*s that are more suitable with respect to S_a for predicting the structural performance such as the spectral acceleration averaged over a period range or vector-valued *IM*s (e.g., Ebrahimian et al. 2015). However, this paper does not focus on selecting the most suitable *IM*.

The structural damage measure herein is taken to be the critical Demand to Capacity Ratio (*DCR*) (Jalayer et al. 2017) for a desired limit state (*LS*), denoted as DCR_{LS}. It is defined as the demand to capacity ratio for the component or mechanism that brings the system closer to the onset of a limit state *LS* (herein, the Near-Collapse limit state). The formulation is based on the cut-set concept (Ditlevsen and Madsen 1996), which is suitable for cases where various potential failure mechanisms (both ductile and brittle) can be defined a priori. DCR_{LS}, which is always equal to unity at the onset of limit state, is defined as:

$$DCR_{LS} = \max_{l}^{N_{mech}} \min_{j}^{N_l} \frac{D_{jl}}{C_{jl}} \quad (1)$$

where N_{mech} is the number of considered potential failure mechanisms; N_l is the number of components taking part in the l^{th} mechanism; D_{jl} is the demand evaluated for the j^{th} structural component of the l^{th} mechanism; C_{jl} is the limit state capacity for the j^{th} component of the l^{th} mechanism. The limit state of Near-Collapse is considered according to Eurocode 8 (CEN 2005). DCR_{LS} takes into account also brittle failure modes such as shear failure in the structural members (see Jalayer et al. 2015 and 2017 for a more detailed description of the defined cut-sets). Such formulation is particularly useful in cases where the non-linear shear behavior is not modeled explicitly at the element level (the case of this work, as it will be explained hereafter). When predicting non-linear response of structures, it is necessary to account for the possibility that some records may cause global "Collapse"; i.e., very high global displacement-based demands or non-convergence problems in the analysis software (see for example Shome and Cornell 1999, Jalayer et al. 2017). Herein, the "collapse-cases" are identified as those cases in which either a numerical non-convergence occurs or the maximum inter-story drift exceeds 10% (to account for global dynamic instability).

1.2. Propagating the ergodic uncertainties: Poissonian limit state excursion

When the limit state excursion can be described by a homogenous Poisson distribution, the probability of at least one limit state excursion in time t can be calculated as:

$$P\left(DCR_{LS}>1;t\right) = 1-\exp\left[-\lambda\left(DCR_{LS}>1\right)\cdot t\right] \quad (2)$$

where $\lambda(DCR_{LS}>1)$ represents the mean annual frequency of exceeding limit state *LS*. $\lambda(DCR_{LS}>1)$ in its turn can be calculated as:

$$\lambda(DCR_{LS}>1) = \int_{\Omega_{S_a}} P\left(DCR_{LS}>1 \mid S_a\right)\left|\mathrm{d}\lambda_{S_a}\right| \quad (3)$$

where $P(DCR_{LS}>1|S_a)$ is the fragility function and λ_{S_a} is the hazard expressed in terms of the mean annual frequency of exceeding a given S_a value. If record-to-record variability constitutes the only source of uncertainty (e.g., neglecting modelling

uncertainties), it can be assumed –neglecting time-dependent deterioration in structural properties– that the limit state excursion is described by a homogenous Poisson distribution. Hence, Eqs. (2) and (3) can be used to calculate the structural reliability. The uncertain parameters that lead to Poissonian limit state excursion are also referred to as *ergodic* uncertain parameters as per Der Kiureghian (2005) and Der Kiureghian and Ditlevsen (2009).

1.3. Propagating the non-ergodic uncertainties

Let the vector $\boldsymbol{\theta}$ represent all the uncertain parameters in a given seismic structural reliability problem. The subset of parameters that do not necessarily lead to Poissonian limit state excursion, are denoted as $\boldsymbol{\theta}_{NE}$ (*non-ergodic* parameters that do not renew with the occurrence of new events and may lead to dependence between different limit state excursion occurrences). Therefore, the probability of at least one limit state excursion in time t in this case can be written as:

$$P(DCR_{LS}>1;t) = \int_{\Omega_{\boldsymbol{\theta}_{NE}}} P(DCR_{LS}>1;t\,|\,\boldsymbol{\theta}_{NE})\, f(\boldsymbol{\theta}_{NE})\,\mathrm{d}\boldsymbol{\theta}_{NE} \quad (4)$$
$$= \int_{\Omega_{\boldsymbol{\theta}_{NE}}} \left(1-\exp\left[-\lambda(DCR_{LS}>1\,|\,\boldsymbol{\theta}_{NE})\cdot t\right]\right) f(\boldsymbol{\theta}_{NE})\,\mathrm{d}\boldsymbol{\theta}_{NE}$$

where $\lambda(DCR_{LS}>1|\boldsymbol{\theta}_{NE})$ represents the mean annual frequency of exceeding limit state *LS* given a specific realization of the vector of non-ergodic parameters $\boldsymbol{\theta}_{NE}$; $f(\boldsymbol{\theta}_{NE})$ is the joint probability density function for vector $\boldsymbol{\theta}_{NE}$ and $\Omega_{\boldsymbol{\theta}_{NE}}$ is the domain of $\boldsymbol{\theta}_{NE}$. $\lambda(DCR_{LS}>1|\boldsymbol{\theta}_{NE})$ can be calculated from Eq. (3) by substituting $P(DCR_{LS}>1|S_a)$ with $P(DCR_{LS}>1|S_a,\boldsymbol{\theta}_{NE})$, where $P(DCR_{LS}>1|S_a,\theta_{NE})$ is the fragility function conditioned on a given realization of the vector of non-ergodic uncertain parameters.

*1.4. Data **D***

The Data **D**, rather than representing observed data, herein represents the damage measure values calculated for several simulations N_{sim} of the vector of uncertain parameters $\boldsymbol{\Theta}$. More specifically, data **D**, in the ergodic case (only record-to-record variability as the source of uncertainty) represents the pairs of (DCR_{LS}, S_a) values for a set of N ground motion records (N_{sim}=N). In case the structural modelling uncertainties are also considered (the non-ergodic case), **D** represents the vector containing the pair of (DCR_{LS}, S_a) values in two different configurations: (a) each record is applied to a different realization of the structural model (i.e., the one-to-one assignment); note that the number of simulations N_{sim} is equal to the number of records N (used for the case in which the Poisson formulas are applied for calculating risk from Eqs. 2 and 3); (b) each set of N (DCR_{LS}, S_a) pairs, denoted herein as $\mathbf{D}(\boldsymbol{\theta}_m)$, corresponds to a different realization of the structural model $\boldsymbol{\theta}_m$ (a subset of non-ergodic uncertain parameters $\boldsymbol{\theta}_{NE}$); i.e., N_{sim} is equal to the product of the number of records N and the number of structural model realizations $N_{\mathcal{M}}$. (used for the general case in which Eq (4) is employed for calculating the risk).

1.5. Robust fragility

Inspired from the concept of updated robust reliability (Beck and Au 2002), predictive fragilities (Sasani and Der Kiureghian 2001) and average fragilities (Kennedy and Ravindra 1983), the Robust Fragility is defined as the expected value for a prescribed fragility model considering the joint probability distribution for the (fragility) model parameters. The Robust Fragility can be expressed as:

$$P\left(DCR_{LS}>1\,\middle|\,S_a,\mathbf{D}\right) = \quad (5)$$
$$\int_{\Omega_{\boldsymbol{\chi}}} P\left(DCR_{LS}>1\,\middle|\,S_a,\boldsymbol{\chi}\right) f(\boldsymbol{\chi}\,|\,\mathbf{D})\,\mathrm{d}\boldsymbol{\chi} =$$
$$\mathbb{E}_{\boldsymbol{\chi}|\mathbf{D}}\left[P\left(DCR_{LS}>1\,\middle|\,S_a,\boldsymbol{\chi}\right)\right]$$

where $\boldsymbol{\chi}$ is the vector of fragility model parameters (e.g., median and standard deviation of the logarithm for the Lognormal Distribution) and $\Omega_{\boldsymbol{\chi}}$ is its domain; $f(\boldsymbol{\chi}|\mathbf{D})$ is the joint probability distribution for fragility model parameters given the vector of data **D** (see Section 1.4). The term $P(DCR_{LS}>1|S_a,\boldsymbol{\chi})$ is the fragility function given that the vector $\boldsymbol{\chi}$ is known. $\mathbb{E}_{\boldsymbol{\chi}|\mathbf{D}}(\cdot)$ is the expected value over the vector of fragility parameters $\boldsymbol{\chi}$. It has been assumed that, once conditioned on fragility parameters $\boldsymbol{\chi}$, the fragility is independent

of data **D**. The variance $\sigma^2_{\chi|\mathbf{D}}$ in fragility estimation can be calculated as:

$$\sigma^2_{\chi|\mathbf{D}}\left[P\left(DCR_{LS}>1|S_a,\boldsymbol{\chi}\right)\right]= \mathbb{E}_{\chi|\mathbf{D}}\left[P\left(DCR_{LS}>1|S_a,\boldsymbol{\chi}\right)^2\right] -\left(\mathbb{E}_{\chi|\mathbf{D}}\left[P\left(DCR_{LS}>1|S_a,\boldsymbol{\chi}\right)\right]\right)^2 \quad (6)$$

Note that calculating the variance in fragility estimation $\sigma^2_{\chi|\mathbf{D}}(\cdot)$, provides the possibility of estimating a confidence interval for the fragility considering the uncertainty in the estimation of the fragility model parameters. It should be mentioned that the fragility model parameters $\boldsymbol{\chi}$ are non-ergodic (a subset of $\boldsymbol{\theta}_{NE}$) and probability of limit state excursion –strictly speaking-- should be calculated according to Section 1.3.

1.6. The updated Robust Reliability

In the specific case when $\boldsymbol{\theta}_{NE}=[\boldsymbol{\theta}_m,\boldsymbol{\chi}]$, the Robust updated reliability in Eq. (4) can be written as:

$$\begin{aligned}&P\left(DCR_{LS}>1;t\,|\,\mathbf{D}\right)=\\&\int_{\Omega_{\boldsymbol{\chi}}}\int_{\Omega_{\boldsymbol{\theta}_m}} P\left(DCR_{LS}>1;t\,|\,\boldsymbol{\theta}_m,\boldsymbol{\chi}\right) f\left(\boldsymbol{\chi}\,|\,\boldsymbol{\theta}_m,\mathbf{D}(\boldsymbol{\theta}_m)\right) f(\boldsymbol{\theta}_m)\,\mathrm{d}\boldsymbol{\chi}\,\mathrm{d}\boldsymbol{\theta}_m\\&=\int_{\Omega_{\boldsymbol{\chi}}}\int_{\Omega_{\boldsymbol{\theta}_m}}\left(1-\exp\left[-\lambda\left(DCR_{LS}>1\,|\,\boldsymbol{\theta}_m,\boldsymbol{\chi}\right)t\right]\right) f\left(\boldsymbol{\chi}\,|\,\boldsymbol{\theta}_m,\mathbf{D}(\boldsymbol{\theta}_m)\right) f(\boldsymbol{\theta}_m)\,\mathrm{d}\boldsymbol{\chi}\,\mathrm{d}\boldsymbol{\theta}_m\\&=\mathbb{E}_{\boldsymbol{\theta}_m,\boldsymbol{\chi}|\mathbf{D}}\left[1-\exp\left[-\lambda\left(DCR_{LS}>1\,|\,\boldsymbol{\theta}_m,\boldsymbol{\chi}\right)\cdot t\right]\right]\end{aligned} \quad (7)$$

where $\boldsymbol{\chi}$ is the vector of fragility model parameters and $\Omega_{\boldsymbol{\chi}}$ is its domain; $f(\boldsymbol{\chi}|\boldsymbol{\theta}_m,\ \mathbf{D}(\boldsymbol{\theta}_m))$ is the joint probability distribution for fragility model parameters given the vector of data **D** (see Section 1.4) and a given realization of $\boldsymbol{\theta}_m$. The term $P(DCR_{LS}>1;t|\boldsymbol{\theta}_m,\boldsymbol{\chi})$ is the probability of at least one limit state excursion in time t given that the vectors $\boldsymbol{\chi}$ and $\boldsymbol{\theta}_m$ are known. The term $\lambda(DCR_{LS}>1|\boldsymbol{\chi},\boldsymbol{\theta}_m)$ is the rate of limit state excursion given $\boldsymbol{\chi}$ and $\boldsymbol{\theta}_m$; this term can be calculated as the integral of fragility $P(DCR_{LS}>1|S_a,\boldsymbol{\chi},\boldsymbol{\theta}_m)$ multiplied by $\mathrm{d}|\lambda(S_a)|$ (similar to Eq. 3). Note that it assumed that once conditioned on fragility model parameters $\boldsymbol{\chi}$, the fragility and limit state excursion rate do not depend on data **D**. The variance σ^2 can be calculated as:

$$\begin{aligned}&\sigma^2\left[P\left(DCR_{LS}>1;t\,|\,\mathbf{D}\right)\right]=\mathbb{E}_{\boldsymbol{\theta}_m,\boldsymbol{\chi}|\mathbf{D}}\left[\left(1-\exp\left[-\lambda(DCR_{LS}>1\,|\,\boldsymbol{\theta}_m,\boldsymbol{\chi})\cdot t\right]\right)^2\right]\\&-\left(\mathbb{E}_{\boldsymbol{\theta}_m,\boldsymbol{\chi}|\mathbf{D}}\left[1-\exp\left[-\lambda(DCR_{LS}>1\,|\,\boldsymbol{\theta}_m,\boldsymbol{\chi})\cdot t\right]\right]\right)^2\end{aligned} \quad (8)$$

1.7. Cloud Analysis considering the collapse-cases

A modified version of the Cloud Analysis introduced in Jalayer et al. (2017) is employed (hereafter referred to as Modified Cloud Analysis, MCA). The MCA formally considers the structural response to collapse-inducing records, signaled herein by occurrence of very large *DCR* values, or non-convergence in the analyzing software. Let the Cloud data, that is the pairs of (DCR_{LS}, S_a) for the suite of selected records, be partitioned into two parts: (a) *NoC* data which corresponds to that portion of the suite of records for which the structure does not experience "Collapse", (b) *C* data corresponding to the "Collapse"-inducing records. The structural fragility for a prescribed *LS* can be expanded with respect to *NoC* and *C* sets using Total Probability Theorem (see also Shome and Cornell 1999):

$$\begin{aligned}&P\left(DCR_{LS}>1|S_a\right)=P\left(DCR_{LS}>1|S_a,NoC\right)\cdot\left(1-P(C|S_a)\right)\\&+P\left(DCR_{LS}>1|S_a,C\right)\cdot P\left(C|S_a\right)\end{aligned} \quad (9)$$

where $P(DCR_{LS}>1|S_a,NoC)$ is the conditional probability that DCR_{LS} is greater than unity given that "Collapse" has not taken place (*NoC*) and can be described by a Lognormal distribution (a widely used assumption that has been usually verified for cases where the regression residuals represent unimodal behavior, e.g., Shome et al. 1998):

$$P\left(DCR_{LS}>1|S_a,NoC\right)=\Phi\left(\frac{\ln\eta_{DCR_{LS}|S_a,NoC}}{\beta_{DCR_{LS}|S_a,NoC}}\right) \quad (10)$$

where $\eta_{DCR_{LS}|S_a,NoC}=a\cdot S_a^{\,b}$ and $\beta_{DCR_{LS}|S_a,NoC}$ are conditional median and standard deviation (dispersion) of the natural logarithm of DCR_{LS} for *NoC* portion of the data (a and b are least squares logarithmic linear regression coefficients). $P(DCR_{LS}>1|S_a,NoC)$ is calculated in exactly the same manner as the standard Cloud Analysis. The term $P(DCR_{LS}>1|S_a,C)$ is the conditional probability of that DCR_{LS} is greater than unity given "Collapse". This term is equal to unity in the cases of "Collapse"; i.e., the limit state *LS* (herein, Near-Collapse) is certainly exceeded. Finally, the probability of collapse $P(C|S_a)$ in Eq.

(9), which can be predicted by a logistic regression model (a.k.a., logit) as a function of S_a (see also Jalayer and Ebrahimian 2017), is expressed as follows:

$$P(C|S_a) = \frac{1}{1+e^{-(\alpha_0+\alpha_1 \cdot \ln(S_a))}} \quad (11)$$

where α_0 and α_1 are the parameters of the logistic regression.

2. APPLICATION

One of the frames in an existing school (Fig. 1) structure located in Avellino, Italy is considered for the application.

2.1. The structural model

The case-study structure consists of three stories with a semi-embedded story and lies on Eurocode 8 (CEN 1998) soil type B. The building is constructed in the 1960s and is designed for gravity loads only. The structure is composed of bi-dimensional parallel frames, without transversal beams. The main central frame in the structure is used herein as structural model (Fig. 1). The columns have rectangular sections with the following dimensions: first storey, 40×55cm^2, second storey 40×45cm^2, third storey, 40×40cm^2, and forth storey, 30×40cm^2. The beams, also with rectangular section, have the following dimensions: 40×70cm^2 at first and second storey, and 30×50cm^2 for the ultimate two floors. The finite element model of the frame is constructed, using OpenSees (http://opensees.berkeley.edu), assuming that the non-linear behaviour in the structure is concentrated in plastic hinges (see Jalayer et al. 2015 for more information about the structural model). The Beam-with-hinges element from the library of OpenSees is used to model the member-end plasticity. As the uniaxial material from OpenSees library, Pinching4 is used. The points on the backbone curve are defined as cracking, yielding, and the peak point, respectively. The coordinates of the peak point are the ultimate bending moment and the 75% of the ultimate curvature. The first two vibration periods for the considered 2D frame are 0.727 and 0.257 seconds.

2.2. The Data **D**

The record-to-record variability is represented herein as the Data **D**. Therefore, the suite of selected ground motions is treated as data. The records need not necessarily be generated from a probability distribution. This aspect is particularly helpful when working with registered ground motion.

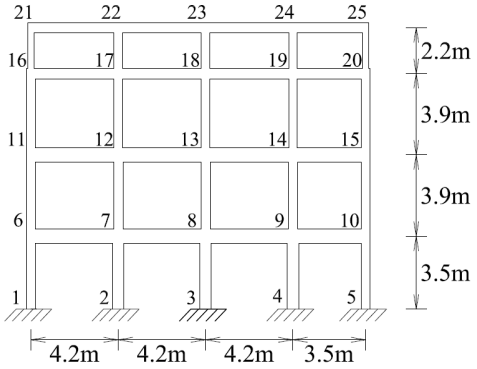

Figure 1: The moment-resisting frame considered in the application

2.2.1. The set of ground motion records

N=90 as-recorded ground motion records are considered herein as a combination of the 20 ground motions in Jalayer et al. (2015) and the 70 ground motions in (Jalayer et al. 2017). It is to note that both records sets (that present no common records) are selected for Cloud Analysis and are intended to span a wide range of intensities. The set of 20 ground motions are recorded on stiff soil (400m/s<V_{s30}<700m/s) which is consistent with the Eurocode 8 (CEN 1998) soil type B (the soil type for the site of the case study). The set of 70 records are selected from the Next Generation of Attenuation (NGA)-West2 database and are recorded on (NEHRP) site classes C-D (180 m/s<V_{s30}<760 m/s). Fig. 2 shows the pseudo-spectral acceleration spectra for the suite of records.

2.3. The non-ergodic uncertain parameters

Non-ergodic uncertainties considered in this work can be classified as model parameter uncertainties. They include the vector of fragility model parameters $\boldsymbol{\chi}$=[ln$a$, b, $\beta_{DCR_{LS}|Sa,NoC}$, α_0, α_1] and the vector of structural modelling parameters $\boldsymbol{\theta}_m$. The latter consists of two categories of

parameters namely: (1) those representing the uncertainties in the component capacities; (2) those representing the uncertainties in mechanical material properties and the structural construction details (herein, stirrup spacing).

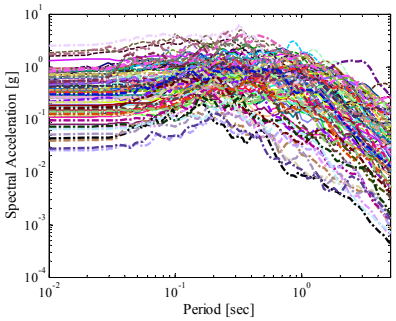

Figure 2: Pseudo acceleration spectra for the 90 as-recorded ground motions

2.3.1. The uncertainty in component capacities

Component capacities are modelled herein as the product of predictive formulas η_{Ci} and unit-median Log Normal variables ε_{Ci} (with logarithmic standard deviation equal to σ_{Ci}) accounting for the uncertainty in component capacity (as described in Jalayer et al. 2007 and 2015). It is assumed that the deviations ε_{Ci} from the predictive formulas are fully-correlated across the entire frame for each type (i.e., yield rotation, ultimate rotation and shear capacity).

2.3.2. Uncertainties in the mechanical material properties and the construction details

The parameters identifying the probability distributions for the material mechanical properties (concrete strength and steel yielding force) have been based on the values typical of the post-world war II construction in Italy (see Jalayer et al. 2015 for more details). It is assumed that the material properties are fully correlated across each floor and uncorrelated between different floors.

Stirrup spacing in the beams and columns is assumed to be the only source of uncertainty related to construction details. Having a presumably shear-critical structure, the spacing of the shear rebar is expected to affect significantly the seismic structural behavior. It is assumed that the information about the shear rebar is limited to the knowledge of stirrup diameter (equal to 6 mm), and the intervals in which the stirrup spacing is supposed to vary (the minimum values for stirrup spacing are equal to those specified in the original design documents and maximum values are loosely based the maximum admissible stirrup spacing according to the code). Hence, a uniform distribution is assumed in the interval formed by the minimum and the maximum values (Jalayer et al. 2015). It is assumed that the stirrup spacing values are fully correlated across beam and columns (considering no cross-correlation between the stirrup spacing in beams and columns).

2.4. Robust reliability estimation using simulation

The Robust fragility curve and its standard deviation in Eqs. (5-6) and the updated robust reliability in Eqs. (7-8) can be calculated efficiently using Monte Carlo Simulation (see also Jalayer et al. 2017). Herein, an advanced simulation scheme known as Markov Chain Monte Carlo (MCMC) simulation is employed in order to directly sample from the posterior joint PDFs $f(\boldsymbol{\chi}|\mathbf{D})$ and $f(\boldsymbol{\chi}|\mathbf{D}(\boldsymbol{\theta}_m), \boldsymbol{\theta}_m)$ where $\boldsymbol{\chi}=[\ln a, b, \beta_{DCR_{LS}|Sa,NoC}, \alpha_0, \alpha_1]$.

2.5. The results

Fig. 3 demonstrates the data **D** corresponding to the Modified Cloud Analysis (MCA) when structural modelling parameters $\boldsymbol{\theta}_m$ are considered (following option (a) described in Section 1.4). This dataset consists of the pairs of (DCR_{LS}, S_a) for the suite of N_{sim}=90 as-recorded ground motion records for the limit state of Near Collapse. Note that each record is applied to one of i=1:$N_{\mathcal{M}}$ realizations of the structural model (the total number of structural analyses performed is $N_{sim}=N_{\mathcal{M}}$=90). The non-collapse (NoC) data pairs are plotted as blue circles and the "collapse" data pairs are plotted as red circles. The figure shows in dashed grey line the linear regression fitted in the logarithmic scale to the non-collapse portion of the data. The figure also shows the median prediction based on both linear and logistic regression considering the "collapse" portion of

data (solid grey line). The MCA analysis also provides the histogram for linear regression residuals for the non-collapse portion of data. The histogram seems to visually justify the assumption of Normal logarithmic regression residuals.

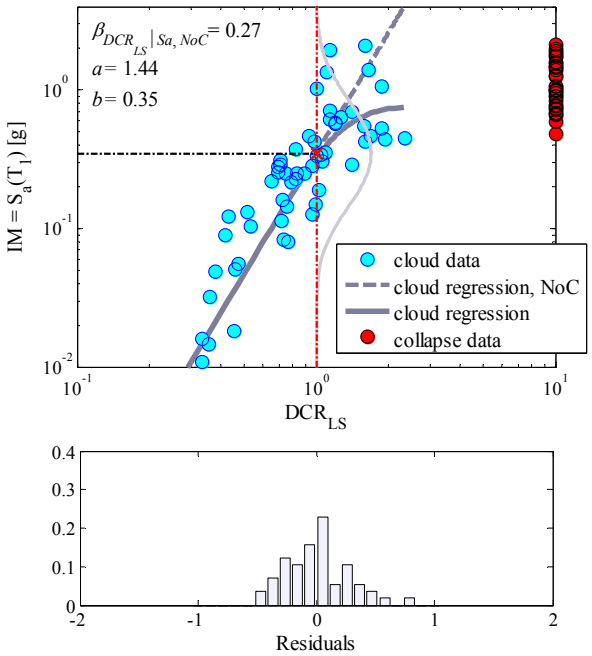

Figure 3: Modified Cloud Analysis (MCA) for data pairs (DCR_{LS}, S_a) considering record-to-record variability and structural modelling uncertainties

Fig. 4 demonstrates the robust fragility curve $P(DCR_{LS}>1|S_a, \mathbf{D})$ (from Eq. 5, thick black solid line) and the robust fragility plus/minus one standard deviation (from Eq. 6) curve (the grey area) for the case were both structural modelling uncertainties $\boldsymbol{\theta}_m$ and record-to-record variability are considered (based on data **D** plotted in Fig. 3). The figure also demonstrates the robust fragility (blue solid line) and the robust fragility plus/minus one standard deviation curves (dashed blue lines) for the case where only record-to-record variability is considered. The fragility curve considering the structural modeling uncertainties seems to follow the expected trends with respect to the fragility curve without the consideration of modeling parameter uncertainties; namely, reduced median and increased dispersion.

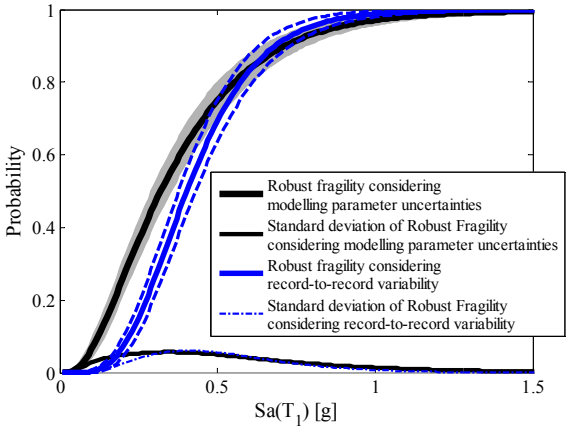

Figure 4: The robust fragility and the robust fragility plus/minus one standard deviation

Fig. 5 represents the probability of at least one limit state excursion, when modelling parameter uncertainties are considered (i.e., $\boldsymbol{\theta}_{NE}=[\boldsymbol{\theta}_m,\boldsymbol{\chi}]$), calculated as updated reliability in Eq. (7) in thick soli grey line and its plus/minus one standard deviation interval (the grey area) as in Eq. (8). The black lines represent the limit state excursion according to Eq. (2) for the very efficient robust fragility curve (Eq. 5) plotted in solid lines and the limit state excursion probabilities corresponding to the robust fragility plus/minus one standard deviation (Eq. 6) --based on data on data **D** as in option (a) in Section 1.4 ($N_{sim}=N$).

The robust updated reliability and its plus/minus one standard deviation confidence interval, when only record-to-record variability and the fragility model parameter uncertainties are considered (Eqs. 7-8 considering only $\boldsymbol{\theta}_{NE}=[\boldsymbol{\chi}]$), are plotted as blue dashed-dot and dashed lines, respectively.

It can be observed that employing the very efficient ($N_{sim}=N$) robust fragility concept, provides reliability estimates within plus one standard deviation of the more rigorous and more computationally intensive robust updated reliability. However, it underestimates the uncertainties in reliability estimation (the confidence band is significantly "narrower" than the rigorous case). However, this aspect needs to be further investigated for larger $N_{\mathcal{M}}$ values.

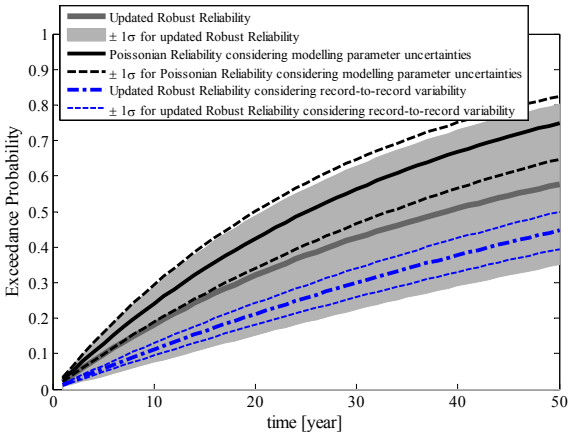

Figure 5: The updated robust reliability and its plus/minus one standard deviation interval

3. CONCLUSIONS

The paper discusses robust reliability assessment considering the uncertainties in the fragility model parameters, the structural modelling parameter uncertainties and record-to-record variability based on registered records. It is demonstrated that a very efficient method based on the robust fragility concept –implicitly assuming ergodic type of uncertainties-- leads to conservative estimates of limit state excursion probability within plus one standard deviation of the robust reliability calculated through explicit treatment of non-ergodic uncertainties.

4. REFERENCES

Beck, J.L. and Au, S.K. (2002). Bayesian updating of structural models and reliability using Markov chain Monte Carlo simulation. *Journal of engineering mechanics*, 128(4), pp.380-391.

CEN (2004). *Eurocode 8: design of structures for earthquake resistance. Part 1: General rules, seismic actions and rules for buildings*. EN 1998-1 CEN Brussels: April 2004.

Der Kiureghian, A. (2005). "Non-ergodicity and PEER's framework formula." *Earthquake engineering & structural dynamics*, 34(13), 1643-1652.

Der Kiureghian, A. and Ditlevsen, O. (2009). Aleatory or epistemic? Does it matter?. *Structural Safety*, 31(2), pp.105-112.

Ditlevsen O, Madsen HO. (1996) *Structural reliability methods*. Wiley: New York.

Ebrahimian, H., Jalayer, F., Lucchini, A., Mollaioli, F. and Manfredi, G. (2015). Preliminary ranking of alternative scalar and vector intensity measures of ground shaking. *Bulletin of Earthquake Engineering*, 13(10), pp.2805-2840.

Jalayer, F., De Risi, R., & Manfredi, G. (2015). Bayesian Cloud Analysis: efficient structural fragility assessment using linear regression. *Bulletin of Earthquake Engineering*, 13(4), 1183-1203.

Jalayer, F., Ebrahimian, H., Miano, A., Manfredi, G. and Sezen, H. (2017). Analytical fragility assessment using unscaled ground motion records. *Earthquake Engineering & Structural Dynamics*, 46(15), pp.2639-2663.

Jalayer F., Ebrahimian H. (2017). Seismic risk assessment considering cumulative damage due to aftershocks. *Earthquake Engineering and Structural Dynamics*, 46(3): 369-389.

Kennedy, R.P. and Ravindra M.K. (1983), Seismic Fragilities for Nuclear Power Plant Risk Studies, *Proceedings of the second CNSI specialist meeting on probabilistic methods in seismic risk assessment for nuclear power plants*.

Miano, A., Jalayer, F. and Prota, A. (2017). Considering structural modeling uncertainties using Bayesian cloud analysis. *In Proceedings of the 6th ECCOMAS Thematic Conference on Computational Methods in Structural Dynamics and Earthquake Engineering* (*COMPDYN*).

Papadimitriou, C., Beck, J. L., & Katafygiotis, L. S. (2001). Updating robust reliability using structural test data. *Probabilistic engineering mechanics*, 16(2), 103-113.

Sasani, M. and Kiureghian, A.D. (2001). Seismic fragility of RC structural walls: displacement approach. *Journal of Structural Engineering*, 127(2), pp.219-228.

Shome, N., Cornell, C. A., Bazzurro, P., & Carballo, J. E. (1998). Earthquakes, records, and nonlinear responses. *Earthquake Spectra*, 14(3), 469-500.

Shome N, Cornell CA (1999). *Probabilistic seismic demand analysis of nonlinear structures*. Report No. RMS35, Stanford University, CA, 320 pp.